nature neuroscience

Task-specific signal transmission from prefrontal cortex in visual selective attention

Yosuke Morishima[1], Rei Akaishi[1], Yohei Yamada[1], Jiro Okuda[2], Keiichiro Toma[1] & Katsuyuki Sakai[1]

Our voluntary behaviors are thought to be controlled by top-down signals from the prefrontal cortex that modulate neural processing in the posterior cortices according to the behavioral goal. However, we have insufficient evidence for the causal effect of the top-down signals. We applied a single-pulse transcranial magnetic stimulation over the human prefrontal cortex and measured the strength of the top-down signals as an increase in the efficiency of neural impulse transmission. The impulse induced by the stimulation transmitted to different posterior visual areas depending on the domain of visual features to which subjects attended. We also found that the amount of impulse transmission was associated with the level of attentional preparation and the performance of visual selective-attention tasks, consistent with the causal role of prefrontal top-down signals.

It is generally accepted that top-down signals from the prefrontal cortex are important for cognitive control[1–4]. The signals are thought to be causal to the task-dependent modulation of neural activity in the posterior cortices and facilitate the processing of task-relevant information[5–7]. This idea is supported by the time precedence of prefrontal activity[8,9], correlation of activity between the prefrontal and posterior regions[10–12] and modulation of activity in the posterior regions after prefrontal inactivation[13–17]. The current evidence is, however, insufficient to prove the causal relationship because it does not necessarily indicate the direct influence of the prefrontal signals over the posterior regions. Other studies have shown that microstimulation to the frontal eye field (FEF) in monkeys modulates neural responses in a posterior visual area within 40 ms of the stimulation, consistent with direct transmission of neural impulse from the FEF[18,19]. It has also been shown that stimulation of the human FEF modulates the excitability of neurons in the human visual motion sensitive area (hMT+) at a latency of 20–40 ms[20]. However, the task-specific nature of the physiological top-down signals remains open because the behavioral task was not manipulated in these studies. Also, the behavioral relevance of the physiological signals can not be tested.

Here, we used transcranial magnetic stimulation (TMS) as a probe to examine the efficiency of the neural impulse transmission from the prefrontal cortex to posterior regions. The rationale for this technique is that stimulation to a neuronal population in a source region induces a current spread toward the anatomically connected target regions and that the direction and the amount of the current spread are modulated depending on the functional status of the neural network, which is determined by the task at hand. Using a cue-based visual feature attention task, we found that the neural impulse from the FEF induced by TMS was transmitted to different posterior visual areas depending on the attended visual features.

RESULTS

Behavior

We asked normal human subjects to perform a visual-discrimination task for motion direction or face gender. The visual target consisted of a vertical grating moving toward the right or left, superimposed on an image of a male or female face (**Fig. 1a**). A task-instruction cue preceded the target with a long or short cue-target interval (CTI, stimulus onset asynchrony of 1,500 or 150 ms, respectively). On half of the trials, we applied a single-pulse TMS at 134 ms after the onset of a visual target over the scalp position at electrode FC2, which was located above the junction of the precentral sulcus and superior frontal sulcus in most subjects (**Fig. 1b**). The mean coordinate of the stimulated region on the cortical surface was (29, –4, 63) based on the MNI (Montreal Neurological Institute) standard brain, which corresponds to the human FEF[21].

The response time of the subjects for the visual-discrimination task did not differ significantly depending on the feature of the target to which the subjects attended ($F_{1,12} = 0.0007$, $P = 0.93$; **Supplementary Fig. 1** online). The response time was significantly shorter on trials with long CTI compared with trials with short CTI, indicating behavioral preparation effect ($F_{1,12} = 35.23$, $P < 0.0001$). The interaction between the feature and CTI was not significant ($F_{1,12} = 2.1$, $P = 0.16$). As for the accuracy of performance, there was a significant main effect of attended feature, with higher accuracy for the face task ($F_{1,12} = 9.93$, $P = 0.008$). The main effect of CTI and the interaction between the feature and CTI were not significant (CTI main effect: $F_{1,12} = 3.64$, $P = 0.08$; interaction effect feature × CTI: $F_{1,12} = 0.49$, $P = 0.49$). Notably, there was no significant main effect of TMS on behavioral performance in terms of response time and accuracy (response time: $F_{1,12} = 0.11$, $P = 0.68$; accuracy: $F_{1,12} = 1.19$, $P = 0.29$). This is because we used low-intensity TMS (80% of the active motor threshold, 27–42% of the

[1]Department of Cognitive Neuroscience, Graduate School of Medicine, University of Tokyo, Hongo 7-3-1, Bunkyo-ku, Tokyo, Japan, 113-0033. [2]Brain Science Institute, Tamagawa University, Tamagawa-gakuen 6-1-1, Machida-shi, Tokyo, Japan, 194-8610. Correspondence should be addressed to K.S. (ksakai@m.u-tokyo.ac.jp).

Received 19 September; accepted 3 November; published online 21 December 2008; doi:10.1038/nn.2237

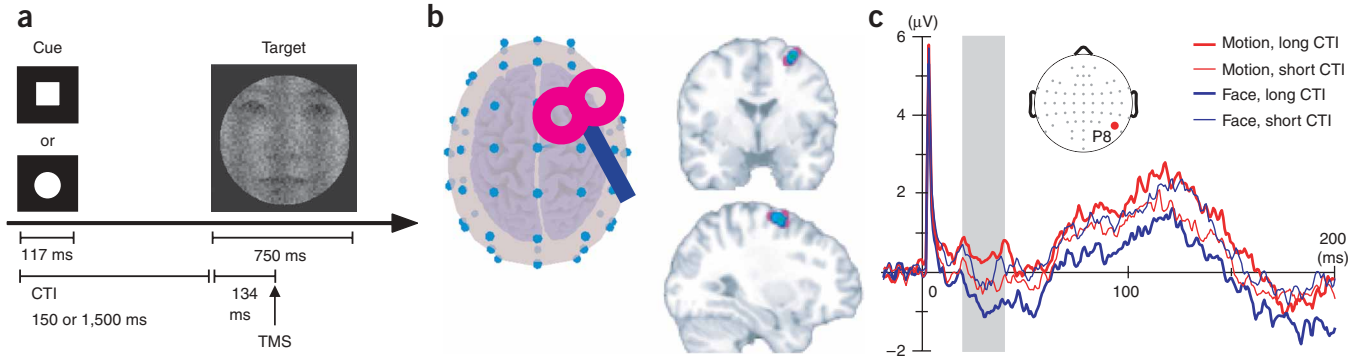

Figure 1 Experimental design and TMS-induced ERP. (**a**) Illustration of the timeline of the behavioral task. Subjects discriminated either the direction of the motion of a vertical grating or the gender of a face on the basis of a cue. The square and circle cues indicate the motion- and face-discrimination tasks, respectively. The stimulus onset asynchrony between the cue and target was either 150 or 1,500 ms. On half of the trials, TMS was given at 134 ms after the onset of a target. (**b**) Left, scalp position and orientation of the TMS coil. Right, location of the TMS site superimposed on the structural image of the MNI template brain. (**c**) Mean TMS-induced ERP at occipito-temporal electrode P8. Red and blue lines indicate the motion and face tasks, respectively. The thick and thin lines indicate trials with long and short CTI, respectively. The shaded region corresponds to the 20–40-ms period after the onset of the TMS. No digital filter was applied to the traces.

maximum output of the stimulator). We used TMS as a probe to examine the effective connectivity of the neuronal network and not as a tool to manipulate the neural processing in the source region. The TMS effect did not interact significantly with feature and CTI in terms of response time (TMS × feature: $F_{1,12} = 2.14$, $P = 0.16$; TMS × CTI: $F_{1,12} = 0.83$, $P = 0.37$) and accuracy (TMS × feature: $F_{1,12} = 0.49$, $P = 0.49$; TMS × CTI: $F_{1,12} = 0.0003$, $P = 0.98$). We also confirmed that the TMS did not induce any detectable saccadic eye movements.

Task-specific TMS effect on EEG potentials

Applying TMS over the right FEF induced changes in the scalp potentials recorded with electroencephalography (EEG). To compare the TMS effect on scalp potentials, we subtracted the event-related potential (ERP) on no TMS trials from that on TMS trials (**Fig. 1c**). The initial TMS effect, as well as the stimulus-related artifacts localized at the stimulation site, was followed by a long-distance TMS effect over the frontal and posterior regions at 20–40 ms after the TMS (**Fig. 2**). The peak of the TMS-induced ERP moved to the vertex region at 40–60 ms and then spread again over the frontal and posterior regions, with maximum changes being observed at 100–120 ms.

The difference in the ERPs of the TMS and no TMS trials cannot be explained by the baseline shift of the ERP before the TMS, as there was no substantial difference in the ERPs during the CTI and the period of time between the target onset and TMS (**Supplementary Fig. 2** online). During an experimental session, the TMS and no TMS trials were given in a pseudo-random order and the subjects were thus unable to anticipate the TMS or the clicking sound that it made. The TMS-induced changes in the scalp potential cannot be explained by the latency shift of ERP components in no TMS trials because there were no corresponding ERP components in no TMS trials. Thus, the differential ERPs between the TMS and no TMS trials was considered to be induced purely by the TMS.

Notably, the TMS-induced ERPs differed between the face and motion conditions when subjects had sufficient time to prepare for the task (long CTI trials). We observed a significant difference ($P < 0.05$) in the TMS-induced ERP at 20–40 ms after TMS over the right posterior parieto-occipital regions (**Fig. 2**). At this time period, the ERP on electrode P8 was positive in the motion condition and was negative in the face condition (**Fig. 1c**). At a later time window of 100–160 ms, there was also a significant difference in ERPs ($P < 0.05$) on the right posterior and central regions. Notably, there was no significant difference ($P > 0.05$) in the TMS-induced ERP in posterior cortical regions between the two conditions until 80 ms after the TMS on trials with short CTI, in contrast with the feature-specific TMS-induced ERP on trials with long CTI (**Fig. 2**). More specifically, there was a significant interaction ($P < 0.05$) between the task condition and CTI over the right posterior parieto-occipital region at 20–40 ms after the TMS (**Fig. 2**). This trend was also observed at 0–20 ms, but disappeared after 40 ms.

We considered the possibility that the spread pattern of the TMS-induced activation on trials with short CTI reflects anatomical connections with the FEF and that functional connectivity reflects task components that are nonspecific to the attended visual feature. In contrast, this pattern of functional connectivity is modulated by the task components that are specific to the attended visual feature on the long CTI trials. To isolate the attention-related modulation, we subtracted the TMS-induced ERPs on short CTI trials from those on long CTI trials. We focused on the ERPs at 20–40 ms after TMS because the transmission of neural impulse from one cortical region to another has been shown to occur in this time range at a neuronal population level[20,22–24]. In the motion task, we observed the modulation of the TMS-induced ERP as a positive deflection of the ERP centered over the temporal to occipital regions (**Fig. 3** and **Supplementary Fig. 3** online). In contrast, we observed the modulation in the face task as a negative deflection of the ERP centered over the right parietal region and a positive deflection centered over the frontal region (z score map in **Fig. 3**). These differential maps of scalp topography reflect the task-dependent functional modulation in the pattern of cortical impulse transmission from the FEF. Notably, the difference between the motion and face conditions was not just the magnitude or the polarity of scalp potential in a localized region, but was instead the spatial pattern of the scalp potential, which suggests different sources for the task-specific ERP modulations.

Task-specific TMS effect on current source densities

The idea of different sources for the ERP modulations was confirmed by the task-specific pattern in the cortical distribution of the current source densities that account for the ERP changes at 20–40 ms after the TMS. We first estimated current source density for the TMS-induced ERP on long CTI trials by using low-resolution electromagnetic tomography (LORETA)[25]. Among the source regions identified in frontal, parietal and temporal cortices, we found higher current source

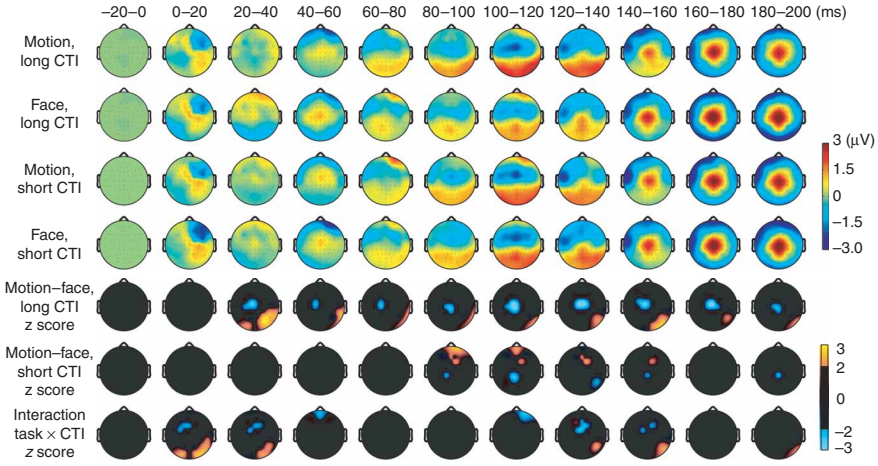

Figure 2 Scalp maps of the TMS effect on ERP. The top four rows show the time course of the mean voltage scalp maps for the TMS effect on the ERP, which are calculated by subtracting the ERP on no TMS trials from the ERP on TMS trials. The maps are shown separately for each of the long and short CTI and motion and face tasks. The fifth and sixth rows show the scalp distribution of the *z* scores representing the difference between the motion and face conditions for each of the long and short CTI trials. The positive sign of the *z* score indicates more positive potentials in the motion compared with the face condition. The bottom row shows the interaction effect between attended feature and CTI. The *z* score is shown in color only when the *P* value at each electrode reached significance ($P = 0.05$).

density in the lateral temporo-occipital region in the motion condition compared with the face condition (**Fig. 4a**). The change was more pronounced on the right hemisphere, which was the side on which TMS was induced. The maximal difference in the current source density was located at coordinate (53, –67, 8), which corresponds to the hMT+[26]. In contrast, there was an increase in the current source density in the inferior temporal cortex in the face condition compared with the motion condition, which was more pronounced on the right side. The maximal difference was found at (46, –53, –20), which corresponds to the human fusiform face area (FFA)[27]. Thus, stimulation of the FEF induced an increase of activity in the hMT+ in the motion condition at 20–40 ms, whereas stimulation induced an increase of activation in the FFA in the face condition at the same latency.

For these task-specific posterior visual areas, we calculated the difference in the current source density between long and short CTI trials for each of the motion and face conditions. These differential current source densities can be viewed as reflecting the modulation of TMS-induced activation in the hMT+ and FFA resulting from attentional preparation. We found a significant region × task interaction on the differential current source densities ($F_{1,12} = 7.594$, $P = 0.017$; **Fig. 4b**), which indicates enhancement of activation in the feature-specific visual areas that are relevant to the task at hand. In fact, the differential activation in the long CTI trials relative to the short CTI trials was significantly larger than zero in task-relevant visual areas ($P = 0.003$), but was not significantly different from zero in task-irrelevant areas ($P = 0.84$) (**Fig. 4b**). The difference between the task-relevant and task-irrelevant areas was significant ($P = 0.017$).

We assumed that the feature-specific pattern of the TMS-induced ERP reflected the efficiency of the neural impulse transmission from the FEF to posterior visual areas. In trials with long CTI, the subjects had sufficient time to prepare for the task and the top-down signals were being sent to the task-specific posterior regions after TMS. In contrast, the subjects were not prepared in trials with short CTI and the task-specific top-down signals were insufficient to modulate the direction of the impulse induced by TMS. We considered the difference in response time between long and short CTI trials to be the result of the level of attentional preparation, which we have shown to be associated with task-specific direction of the TMS-induced impulse transmission.

Association of TMS-induced activation and behavior

This idea is further supported by the relationship between the amount of the TMS-induced ERP changes and behavioral response time. In each of the short and long CTI conditions, we examined whether the variability in response time is associated with across-trial variability in the efficiency of impulse transmission from the FEF to posterior visual areas. We split the trials in each condition into fast- and slow-response trials and calculated the difference in the current source densities between them. For the short-CTI condition, we found that the difference in the current source densities in task-relevant regions were significantly larger than zero, indicating higher activation in these regions in fast-response trials than in slow-response trials ($P = 0.036$; **Fig. 4c**). Notably, we found that the current source densities in areas irrelevant to the task at hand in these trials with short CTI were also significantly higher in fast-response trials compared with slow-response trials; the differential current source density was significantly larger than zero ($P = 0.029$; **Fig. 4c**). Thus, on trials with short preparation time, the amount of impulse transmission from prefrontal to posterior visual areas was associated with behavioral performance, but the direction of impulse transmission was not task dependent. In contrast, the difference in the induced activation between the fast- and slow-response trials in trials with long CTI was not significantly different from zero in both the task-relevant and task-irrelevant areas (relevant, $P = 0.45$; irrelevant, $P = 0.86$; **Fig. 4c**). In these trials, the level of attentional preparation reached a plateau during the long preparation period and the variability in the response time may have been determined by the bottom-up processing of the target image.

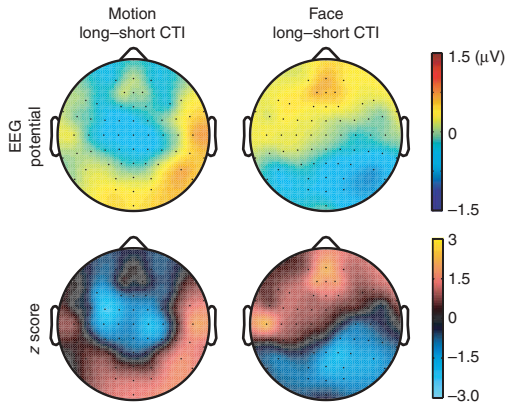

Figure 3 Mean voltage (top) and *z* score (bottom) scalp maps representing the difference between long and short CTI trials at 20–40 ms after TMS. For each of the motion (left) and face conditions (right), the ERP on short CTI trials was subtracted from that on long CTI trials. The positive sign of the *z* scores indicates more positive potential on long CTI compared with short CTI trials.

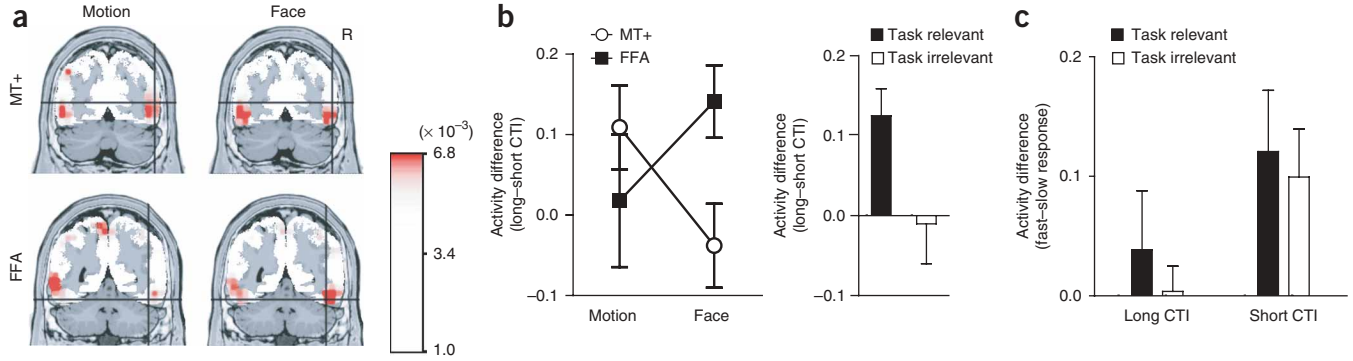

Figure 4 TMS-induced current source density in posterior visual areas. (**a**) Mean TMS-induced current source density at 20–40 ms after TMS on the long CTI trials. The estimated source densities are shown overlaid on the coronal slices of the standard brain at y = –67 (top) and –53 (bottom). The cross-hairs indicate the peak coordinates of the hMT+ (53, –67, 8) (top) and FFA (46 –53 –20) (bottom) at which there was maximal difference in the current source density between the motion and face conditions. R indicates the right side of the brain. (**b**) Left, difference in the current source density between long and short CTI trials in the hMT+ and FFA, shown separately for the motion and face conditions. Right, the difference in the current source density between long and short CTI trials is plotted for the task-relevant (hMT+ for motion task and FFA for face task) and task-irrelevant areas (FFA for motion task and hMT+ for face task). Here the data shown in **a** are log-scaled. Error bars indicate s.e.m. (**c**) Difference in the current source density between fast- and slow-response trials is plotted for task-relevant and task-irrelevant areas, separately for long and short CTI trials. Here the data shown in **a** are log-scaled. Error bars indicate s.e.m.

The difference in the TMS-induced ERP between the fast- and slow-response trials cannot be the result of the nonspecific arousal effect. We examined the pupil diameter of the subjects as an index of arousal level and found that it did not differ significantly between the fast- and slow-response trials. In addition, the global mean field amplitude of the EEG potential induced by the TMS, which has been shown to be associated with arousal level[28], did not differ between the fast- and slow-response trials.

Perturbation of the FEF

Finally, we confirmed that the FEF is important in feature discrimination by disrupting neural processing in the FEF. We applied double-pulse TMS with higher intensity (65% of the maximal output of the stimulator, which was above the active motor threshold for all subjects) while the subjects performed the same motion- or face-discrimination task. The TMS was given at 34 and 134 ms after the target presentation on either the right FEF or the vertex. There was a significant decrease in the accuracy of performance during TMS trials compared with no TMS trials when TMS was given on the FEF ($F_{1,5} = 18.00$, $P = 0.008$), whereas there was no significant effect of TMS when it was given on the vertex control site relative to the no TMS trials ($F_{1,5} = 0.06$, $P = 0.80$) (**Supplementary Fig. 4** online). These results indicate that the FEF is important in the feature-discrimination task, as reported in previous studies[29–32]. Performance had a tendency to be more impaired in the motion task than in the face task (interaction between TMS and task, $F_{1,5} = 6.00$, $P = 0.057$). We also tested the possibility that the perturbation of the right FEF biases the direction of visual motion judgment, but found that the performance did not differ between trials with leftward motion and those with rightward motion; the interaction between TMS and motion direction was not significant (accuracy: $F_{1,5} = 0.14$, $P = 0.72$; response time: $F_{1,5} = 1.836$, $P = 0.23$).

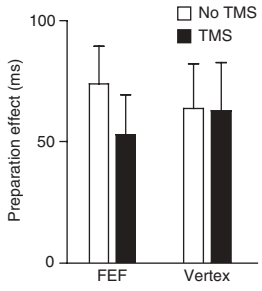

Figure 5 Effect of virtual lesion of the FEF on the behavioral preparation effect. In this experiment, TMS was given with higher intensity at 34 and 134 ms after the onset of target visual image to create a virtual lesion. Left, the preparation effect, which was calculated by subtracting the response time on long CTI trials from that on short CTI trials, is plotted separately for trials with TMS on the right FEF and for trials with no TMS. The data for the motion and face conditions are combined. Right, data for a separate session in which the TMS was applied over the vertex are shown. Error bars indicate s.e.m.

In addition to a decrease in the accuracy of performance, we found that TMS on the FEF diminished the behavioral advantage of a long preparation time (**Fig. 5**). The preparation effect, which was calculated by subtracting the response time on long CTI trials from that on short CTI trials, decreased significantly when TMS was given to the FEF ($t_5 = 2.64$, $P = 0.046$), but it did not change significantly when the TMS was given to the vertex ($t_5 = 0.066$, $P = 0.95$). The effect on preparation was similar for both the motion and face task; the interaction between TMS and task was not significant ($F_{1,5} = 0.69$, $P = 0.44$). The results suggest that the FEF is important for preparation for the feature-discrimination task and that this occurs during the brief time period within 150 ms of target presentation. This finding complements our data on the task-specific pattern of effective connectivity from the FEF observed at the same time period during the long CTI trials. Higher-intensity TMS on the FEF during this time period disrupts the process of establishing task-specific patterns of effective connectivity and thus diminishes the benefit of attentional preparation in speeding up responses.

DISCUSSION

We examined whether the efficiency of a TMS-induced impulse transmission reflects the influence of physiological top-down signals from the FEF over posterior visual areas during visual selective attention. A population of neurons in the FEF that have activity specific to the attended visual feature have been shown to be active before the presentation of a target stimulus[33–35], and these neurons are thought to send top-down signals to neurons in the posterior visual areas that are involved in the processing of that feature[36,37]. In this situation, it can be thought that there is an increase in the responsiveness of the FEF

neurons, projecting to task-relevant visual areas, to the TMS. Also, there is an increase in the responsiveness of neurons in the posterior visual areas to the inputs from the FEF induced by the TMS. Both the pre- and postsynaptic mechanisms reflect the physiological top-down signals from the FEF during visual selective attention and we quantified their effects as a change in the TMS-induced activation in the posterior visual areas. We propose that the TMS-induced ERP in posterior areas reflects mainly orthodromic impulse transmission along the axons of FEF neurons, as scalp EEGs reflect summation of postsynaptic potentials in a local region: EEGs can not detect the firing of posterior visual neurons triggered by antidromic impulse. There still remains the possibility that antidromic firings of neurons may have resulted in organized oscillation in the gamma frequency range in the posterior visual areas[38,39].

FEF neurons have been shown to increase firing in response to a visual stimulus at a specific spatial location or with a specific visual feature[37]. However, the TMS influences the activity of neurons in a region of several centimeters and activates millions of FEF neurons with different preferences for spatial location and visual feature. It remains unknown whether the neural impulse from the FEF at 134 ms after the visual target presentation codes specific information about the target. Here we found that the impulses from the FEF code information about the task that is to be performed, which is the domain of the visual feature to be attended.

The important feature of the top-down control signal is its task-specific nature. We have shown that stimulation of the prefrontal cortex induces activation in posterior visual areas in a manner that is specific to the task at hand. To date, studies have found task-dependent modulation of functional connectivity between the prefrontal and posterior cortices, but these findings tell us nothing about the direction of the influence (**Supplementary Data** and **Supplementary Fig. 5** online)[11,12,40]. Some studies have used mathematical modeling and have estimated the strength of task-specific influence from the prefrontal cortex over the posterior regions, but the estimated values are known to be strongly biased by the arbitrary choice of an anatomical model[40]. Others have used multiple pulses of high-intensity TMS to disrupt neural processing in the frontal or parietal region while subjects performed a visual-attention task[16,17,41]. They found changes in EEG potentials later than 100 ms after the TMS, and it is therefore hard to establish the direct influence of the TMS site over the regions in which the changes in EEG potentials were observed. Also, the effects that were observed in those studies may reflect compensatory mechanisms after the perturbation by TMS.

Our study goes further than previous studies, showing transmission of signals from a specific source region, the FEF, to specific target regions, hMT+ and FFA. Notably, the target regions were identified in an exploratory manner, rather than on the basis of pre-determined regions of interest. In addition, we observed effects at 20–40 ms after TMS, suggesting that there was a direct cortico-cortical impulse transmission from the FEF to the posterior regions[20,22–24], although it remains possible that the effects were instead the result of oligosynaptic impulse transmission. Thus, the functional modulation of the neural circuit that we observed was specific in terms of the source and target and was also specific in terms of the temporal relationship between the cause and effect. TMS-induced current has been shown to spread along anatomical connections from the stimulation site[22] and this can be abolished during sleep[42]. Here, we found a substantial change in the direction of the current spread during voluntary control of attention.

The task-specific patterns in the TMS-induced ERP cannot be accounted for by the difference in the magnitude of regional activation between the face and motion conditions, not only in the FEF, but also in all other cortical regions. On no TMS trials, there was no significant difference in EEG potential between the two task conditions during the time window of 154–174 ms after the target onset, which corresponds to the time window of 20–40 ms after TMS on TMS trials ($P > 0.05$; **Supplementary Fig. 6** online). Thus, the TMS-EEG technique has uncovered changes in effective connectivity, which did not accompany changes in regional activation.

Furthermore, our study found evidence supporting the behavioral importance of the top-down signals. The task-specific modulation of the direction of the impulse transmission from the FEF to posterior visual areas was associated with a behavioral preparation effect, which is determined by the CTI. In addition, the amount of effective impulse transmission from the FEF was associated with across-trial variability in behavioral response on trials with short preparation, which may reflect the level of attentional preparation. However, the regional selectivity of the FEF projection was not observed on trials with short CTI because of insufficient task preparation. In contrast, on trials with long CTI, the effective connectivity from the FEF was directed specifically to the task-relevant visual areas. On these trials, the preparation for the target may have been saturated and the strength of effective connectivity from the FEF did not differ between fast- and slow-response trials. This suggests a mechanism of visual selective attention whereby nonspecific activation of visual neurons is followed by selective activation of task-relevant neurons[43,44]. The tight association with behavior supports our argument that the efficiency in the transmission of the TMS-induced impulse reflects physiological top-down signals that control our voluntary behavior. This idea is also supported by the finding that the perturbation of the FEF with higher-intensity TMS resulted in an increase in errors in the feature-discrimination task and a decrease in the behavioral advantage of long preparation time, which suggests a failure to establish task-specific patterns of effective connectivity.

We have not just shown an association between a single prefrontal region and behavior, but rather have found a tight functional link between a prefrontal region and posterior regions, as well as an association between the prefrontal efferent signals and behavior. Our results also demonstrate the feasibility of our technique for characterizing, at a specific time point of cognitive processing, the functional status of a neural network, which can be dissociated from the pattern of regional activation.

METHODS

Subjects. Fifteen normal subjects (two female, aged 19–26) participated in the TMS-EEG experiments. We excluded two subjects from the analysis as a result of a low correct rate in the motion task (<60%). In addition, six normal subjects (two female, aged 19–32) participated in the TMS-inactivation experiments. All subjects gave written informed consent before participating in this study. The study was approved by the ethics committee of the Graduate School of Medicine at the University of Tokyo.

Cued discrimination task. Subjects were presented with a task instruction cue that was followed by a target stimulus on the black background of a LCD monitor. The target stimulus was a short, 750-ms movie (refresh rate of 60 Hz) with a visual angle of 6 degrees. Each frame of the movie was a composite bitmap image of a vertical sinusoidal grating and a grayscale face image (Softopia Japan Foundation; **Fig. 1a**). A black and white random-noise pattern was also added to the image to equate the behavioral response time between the motion- and face-discrimination tasks. The sinusoidal grating was shifted to the left or right at a speed of 12° s^{-1}. A visual target was preceded by a white square or disc, which instructed the motion- and face-discrimination task, respectively. The duration of the cue presentation was 117 ms and the stimulus onset asynchrony between the cue and target was 150 ms for half of the trials and 1,500 ms for the other half. Subjects responded to the target with a button

press using either the index or middle finger of the right hand. Thus, the task was designed in a two-by-two fashion, (motion and face task) × (long and short CTI). In one experimental session, 20 trials were given for each condition in a pseudo-random order with an intertrial interval of 2–3 s. Each subject was tested in 12 sessions on 2 separate days.

EEG recording and TMS. For each subject, we first determined the threshold intensity of the TMS necessary to evoke motor response. Subjects wore an EEG cap (Nexstim) and were seated on a chair with their hand resting on the desk and their right index finger extended and uplifted. Using a figure eight–shaped flat coil (Magstim 200), we delivered a single-pulse TMS to the scalp position corresponding to the left primary motor cortex (adjusted by moving the coil center in a step of 1 cm) while an electromyographic (EMG) recording was made from the right first dorsal interosseous muscle. The coil was placed tangentially over the scalp, such that the evoked current passed in a posterior to anterior direction in the brain. We defined the active motor threshold as the lowest intensity that evoked more than five small EMG responses (around 50 μV) in a series of ten stimulations.

We then asked the subjects to perform the motion- or face-discrimination task while we recorded EEG from 60 scalp electrodes. The amplifier of the EEG was specially designed to allow TMS pulses to be delivered over the electrode caps (eXimia EEG, Nexstim). This was achieved by closing the circuit for 2 ms on trigger pulse from the magnetic stimulator[22]. We were able to record artifact-free EEG signals 10 ms after the TMS. The EEG signals were referenced to the left ear, filtered at the frequency of 0.1–500 Hz and sampled at 1,450 Hz. To reduce the artifacts resulting from the click sound of the TMS pulse, the subjects wore earplugs.

On half of the trials for each condition, a single-pulse TMS (80% of active motor threshold) was delivered to the right FEF at 134 ms after the onset of the visual target. We chose this time to maximize the difference in the influence of the FEF stimulation between the motion and face tasks. This is based on the finding that the FEF neurons show differential responses to target and distractor at about 100 ms after the presentation of the image in a visual selective-attention task in monkeys[33,34]. It has also been shown that the ERP that is observed at 170 ms after presentation of a face image, called N170, is enhanced when subjects attended to the face[45], suggesting that the top-down signal acts on posterior visual areas at this time period. With a cortico-cortical transmission time of 20–40 ms, we decided that the attentional modulation of the TMS effect would be maximized when the TMS was given over the FEF at ~130 ms after the presentation of a target image. The order of the TMS and no TMS trials was randomized in each experimental session.

The TMS coil was placed tangentially over the FC2 electrode, with the handle of the coil pointing backwards and laterally approximately 45 degrees to the interhemispheric line. After the EEG recording session, the position of the coil was co-registered with the structural magnetic resonance imaging of the brain for each subject using the Brainsight frameless stereotaxy system (Brainsight, Magstim) for 6 of the 15 subjects. In the normalized structural magnetic resonance imaging, the center of the coil was clustered in a spherical region with a diameter of 12 mm across subjects and the mean coordinate of the brain surface just below the coil center was (29, –4, 63) in the MNI space (**Fig. 1b**). This position is considered to be the FEF in the human brain[21]. In a separate session, we also applied TMS on the primary somatosensory cortex (3 cm posterior to hand motor region) in three subjects as control experiments and found that the TMS-induced ERPs did not differ between the motion and face tasks.

Recording eye movement. The pupillary position of the left eye was recorded at 60 Hz with a ViewPoint eye tracker (Arrington Research) and PC-60 software. The eye tracker was adjusted before starting each session. We confirmed that there were no saccadic eye movements between 150 ms before and 300 ms after the presentation of a target. The pupil diameter of the subjects was also recorded at the same sampling rate. The pupil diameter showed a gradual decrease after the presentation of a target, peaking at roughly 500 ms after the presentation. The difference in arousal level is known to affect the pupil size after this light reflex[46]. Thus, the changes in the pupil diameter relative to the pre-target period were calculated and averaged in a time window of 500–800 ms after the target onset and compared between fast- and slow-response trials to see whether the difference in arousal level accounted for the variability in behavioral response speed. We found that the pupil size did not differ between the fast- and slow-response trials.

EEG data analysis. After rejecting trials with blinking and EMG artifacts, we first averaged, for each condition, the ERPs that were time-locked to the onset of the TMS for TMS trials and to the corresponding time point for no TMS trials. We then used EEGLAB[47], implemented on MatLab (Mathworks), for re-reference of the EEG data to an average reference. EEGLAB was also used for statistical analysis and data visualization. After pre-processing, we examined the TMS effect on EEG potentials for each condition by subtracting the ERPs on no TMS trials from those on TMS trials. The baseline of the ERP was corrected with reference to that obtained during the 0–20-ms period before the onset of TMS. Although we used TMS-compatible EEGs, TMS-related artifacts were still observed for a short period after TMS (<10 ms). We also observed artifacts around 200–210 ms after the TMS, when the stimulator started to recharge its energy-storage capacitor after each single-pulse of the TMS. Click sounds associated with the TMS-induced auditory evoked potentials around 80 ms after the TMS[48]. However, we primarily focused on the EEG data collected during the 20–40-ms period after the TMS and consider this period to be free of these artifacts. In addition, as the main aim of our study was to compare the TMS-induced ERP changes across conditions, TMS-induced artifacts do not affect the analysis.

We compared TMS-induced ERPs between face and motion conditions for each of the long and short CTI trials and examined the task-specific modulation of the pattern of neural impulse transmission. We then subtracted, for each of the face and motion conditions, the TMS-induced ERPs on short CTI trials from those on long CTI trials and examined the components of the ERPs that were modulated by the preparation of specific attention tasks.

To obtain the time course of the overall amount of electrical activity induced by TMS, we calculated the global mean field amplitude by the formula

$$\sqrt{\frac{\sum_{i=1}^{N}(V_i-\bar{V})^2}{N}},$$

where N is the number of channels, V_i is the voltage measured with channel i, and $\bar{V}$ is the mean of the measured voltages. This value has been shown to be associated with the arousal level of the subjects[28]

Estimation of current source density. To estimate the cortical distribution of the current source density that accounts for the TMS-induced ERP, we used LORETA[25]. LORETA computes the three-dimensional distribution of neuronal generators of the observed electrical activity in a three-shell spherical head model. The head model includes scalp, skull and brain compartments. The brain compartment was restricted to the cortical gray matter of the standard brain of the MNI, which was resampled to 2,394 cubic voxels at a 7-mm resolution. To determine EEG electrode positions in the brain images, we used previously reported coordinates[49]. In that study, the positions of scalp EEG electrodes were determined on the basis of the cartesian coordinates in the best-fitting sphere, and the position data were merged with the magnetic resonance imaging of the template brain. It was reported that the test-retest variability across subject was, on average, 4.8 mm.

The LORETA functional images represent the electrical activity at each voxel as the squared magnitude (that is, power) of the computed current density. We obtained current source density at each time point for the grand-averaged TMS-induced ERPs across subjects in each condition. We log-scaled and averaged the current source density during the 20–40-ms period after the TMS. We then compared the current source density between the motion and face conditions on trials with long CTI and identified the peak coordinate that showed the maximal difference in the current source density between the two conditions in the middle temporal and fusiform gyrus. Next, we calculated the current source densities for each subject from these peak coordinates on the long and short CTI trials. The difference in the current source densities between the long and short CTI trials was calculated for each region, task and subject, and we applied two-way ANOVA with repeated measures. We also compared the current source densities between task-relevant and task-irrelevant regions using two-tailed paired t tests. Finally, we calculated the difference in the current source densities between the fast- and slow-response trials for each of the long and short CTI trial conditions in the motion and face tasks. We

used one-sample *t* test to examine whether the difference in the current source density between the fast- and slow-response trials was significantly larger than zero.

TMS-perturbation experiments. We used the same motion- and face-discrimination task for our TMS-perturbation experiments as we used in the main TMS-EEG experiments. In one experimental session, 12 trials for each of the four conditions (short- and long-CTI conditions for each of the face and motion tasks) were given in a pseudo-random order with an intertrial interval of 2–3 s. Subjects performed the task for four sessions. On half of the trials, we delivered double-pulse TMS using a figure eight–shaped flat coil (Magstim Rapid) to the scalp position corresponding to the right FEF at 34 and 134 ms after the onset of a visual target. In this experiment, the TMS was used to perturb the neural processing in the FEF. The effect is thought to be mediated by silencing task-related neurons as well as by stimulating neurons that are not related to the task. The order of the TMS and no TMS trials was randomized in an experimental session. The stimulus intensity was set at 65% of maximum output of the stimulator. The same subjects performed the task for another four sessions and a double-pulse TMS of the same intensity was delivered to the vertex in half of the trials. The TMS coil was placed tangentially over the vertex with the handle of the coil pointing backwards and aligned to the interhemispheric line. The TMS did not elicit any saccadic eye movements for both the FEF-TMS and vertex-TMS sessions. For statistical analysis of behavioral data, we carried out three-way ANOVAs (motion or face task, TMS or no TMS and long or short CTI) separately for the FEF-TMS and vertex-TMS sessions.

Note: Supplementary information is available on the Nature Neuroscience website.

ACKNOWLEDGMENTS

We thank M. Okamoto and N. Yamamoto for assistance with EEG recording. This work was supported by a Grant-in-Aid for Scientific Research (A) and a Grant-in-Aid for Young Scientists (S) from the Japan Society for the Promotion of Science, and a Grant-in-Aid from the Center of Excellence Program, Center for Brain Medical Science, from the Ministry of Education, Culture, Sports, Science and Technology, Japan.

AUTHOR CONTRIBUTIONS

Y.M. designed the task, conducted the experiments and analyzed the data. R.A., Y.Y., J.O. and K.T. contributed to the experiments and analysis. K.S. conceptualized the original idea for the study. Y.M. and K.S. wrote the paper.

Published online at http://www.nature.com/natureneuroscience/
Reprints and permissions information is available online at http://npg.nature.com/reprintsandpermissions/

1. Desimone, R. & Duncan, J. Neural mechanisms of selective visual attention. *Annu. Rev. Neurosci.* **18**, 193–222 (1995).
2. Kastner, S. & Ungerleider, L.G. Mechanisms of visual attention in the human cortex. *Annu. Rev. Neurosci.* **23**, 315–341 (2000).
3. Miller, E.K. & Cohen, J.D. An integrative theory of prefrontal cortex function. *Annu. Rev. Neurosci.* **24**, 167–202 (2001).
4. Corbetta, M. & Shulman, G.L. Control of goal-directed and stimulus-driven attention in the brain. *Nat. Rev. Neurosci.* **3**, 201–215 (2002).
5. Moran, J. & Desimone, R. Selective attention gates visual processing in the extrastriate cortex. *Science* **229**, 782–784 (1985).
6. Reynolds, J.H. & Chelazzi, L. Attentional modulation of visual processing. *Annu. Rev. Neurosci.* **27**, 611–647 (2004).
7. Maunsell, J.H. & Treue, S. Feature-based attention in visual cortex. *Trends Neurosci.* **29**, 317–322 (2006).
8. Brass, M., Ullsperger, M., Knoesche, T.R., von Cramon, D.Y. & Phillips, N.A. Who comes first? The role of the prefrontal and parietal cortex in cognitive control. *J. Cogn. Neurosci.* **17**, 1367–1375 (2005).
9. Grent-'t-Jong, T. & Woldorff, M.G. Timing and sequence of brain activity in top-down control of visual-spatial attention. *PLoS Biol.* **5**, e12 (2007).
10. Buchel, C. & Friston, K.J. Modulation of connectivity in visual pathways by attention: cortical interactions evaluated with structural equation modeling and fMRI. *Cereb. Cortex* **7**, 768–778 (1997).
11. Sakai, K. & Passingham, R.E. Prefrontal interactions reflect future task operations. *Nat. Neurosci.* **6**, 75–81 (2003).
12. Sakai, K. & Passingham, R.E. Prefrontal set activity predicts rule-specific neural processing during subsequent cognitive performance. *J. Neurosci.* **26**, 1211–1218 (2006).
13. Fuster, J.M., Bauer, R.H. & Jervey, J.P. Functional interactions between inferotemporal and prefrontal cortex in a cognitive task. *Brain Res.* **330**, 299–307 (1985).
14. Tomita, H., Ohbayashi, M., Nakahara, K., Hasegawa, I. & Miyashita, Y. Top-down signal from prefrontal cortex in executive control of memory retrieval. *Nature* **401**, 699–703 (1999).
15. Barcelo, F., Suwazono, S. & Knight, R.T. Prefrontal modulation of visual processing in humans. *Nat. Neurosci.* **3**, 399–403 (2000).
16. Taylor, P.C., Nobre, A.C. & Rushworth, M.F. FEF TMS affects visual cortical activity. *Cereb. Cortex* **17**, 391–399 (2007).
17. Taylor, P.C., Nobre, A.C. & Rushworth, M.F. Subsecond changes in top down control exerted by human medial frontal cortex during conflict and action selection: a combined transcranial magnetic stimulation electroencephalography study. *J. Neurosci.* **27**, 11343–11353 (2007).
18. Moore, T. & Armstrong, K.M. Selective gating of visual signals by microstimulation of frontal cortex. *Nature* **421**, 370–373 (2003).
19. Armstrong, K.M. & Moore, T. Rapid enhancement of visual cortical response discriminability by microstimulation of the frontal eye field. *Proc. Natl. Acad. Sci. USA* **104**, 9499–9504 (2007).
20. Silvanto, J., Lavie, N. & Walsh, V. Stimulation of the human frontal eye fields modulates sensitivity of extrastriate visual cortex. *J. Neurophysiol.* **96**, 941–945 (2006).
21. Grosbras, M.H., Laird, A.R. & Paus, T. Cortical regions involved in eye movements, shifts of attention and gaze perception. *Hum. Brain Mapp.* **25**, 140–154 (2005).
22. Ilmoniemi, R.J. *et al.* Neuronal responses to magnetic stimulation reveal cortical reactivity and connectivity. *Neuroreport* **8**, 3537–3540 (1997).
23. Pascual-Leone, A. & Walsh, V. Fast backprojections from the motion to the primary visual area necessary for visual awareness. *Science* **292**, 510–512 (2001).
24. Matsumoto, R. *et al.* Functional connectivity in human cortical motor system: a cortico-cortical evoked potential study. *Brain* **130**, 181–197 (2007).
25. Pascual-Marqui, R.D. *et al.* Low-resolution brain electromagnetic tomography (LORETA) functional imaging in acute, neuroleptic-naive, first-episode, productive schizophrenia. *Psychiatry Res.* **90**, 169–179 (1999).
26. Tootell, R.B. *et al.* Functional analysis of human MT and related visual cortical areas using magnetic resonance imaging. *J. Neurosci.* **15**, 3215–3230 (1995).
27. Kanwisher, N., McDermott, J. & Chun, M.M. The fusiform face area: a module in human extrastriate cortex specialized for face perception. *J. Neurosci.* **17**, 4302–4311 (1997).
28. Kahkonen, S. *et al.* Ethanol modulates cortical activity: direct evidence with combined TMS and EEG. *Neuroimage* **14**, 322–328 (2001).
29. Grosbras, M.H. & Paus, T. Transcranial magnetic stimulation of the human frontal eye field: effects on visual perception and attention. *J. Cogn. Neurosci.* **14**, 1109–1120 (2002).
30. Grosbras, M.H. & Paus, T. Transcranial magnetic stimulation of the human frontal eye field facilitates visual awareness. *Eur. J. Neurosci.* **18**, 3121–3126 (2003).
31. O'Shea, J., Muggleton, N.G., Cowey, A. & Walsh, V. Timing of target discrimination in human frontal eye fields. *J. Cogn. Neurosci.* **16**, 1060–1067 (2004).
32. O'Shea, J., Muggleton, N.G., Cowey, A. & Walsh, V. Human frontal eye fields and spatial priming of pop-out. *J. Cogn. Neurosci.* **19**, 1140–1151 (2007).
33. Bichot, N.P. & Schall, J.D. Effects of similarity and history on neural mechanisms of visual selection. *Nat. Neurosci.* **2**, 549–554 (1999).
34. Thompson, K.G. & Bichot, N.P. A visual salience map in the primate frontal eye field. *Prog. Brain Res.* **147**, 251–262 (2005).
35. Peng, X., Sereno, M.E., Silva, A.K., Lehky, S.R. & Sereno, A.B. Shape selectivity in primate frontal eye field. *J. Neurophysiol.* **100**, 796–814 (2008).
36. Stanton, G.B., Bruce, C.J. & Goldberg, M.E. Topography of projections to posterior cortical areas from the macaque frontal eye fields. *J. Comp. Neurol.* **353**, 291–305 (1995).
37. Egner, T. *et al.* Neural integration of top-down spatial and feature-based information in visual search. *J. Neurosci.* **28**, 6141–6151 (2008).
38. Lakatos, P., Chen, C.M., O'Connell, M.N., Mills, A. & Schroeder, C.E. Neuronal oscillations and multisensory interaction in primary auditory cortex. *Neuron* **53**, 279–292 (2007).
39. Lakatos, P., Karmos, G., Mehta, A.D., Ulbert, I. & Schroeder, C.E. Entrainment of neuronal oscillations as a mechanism of attentional selection. *Science* **320**, 110–113 (2008).
40. Horwitz, B. *et al.* Investigating the neural basis for functional and effective connectivity. Application to fMRI. *Phil. Trans. R. Soc. Lond. B* **360**, 1093–1108 (2005).
41. Fuggetta, G., Pavone, E.F., Walsh, V., Kiss, M. & Eimer, M. Cortico-cortical interactions in spatial attention: a combined ERP/TMS study. *J. Neurophysiol.* **95**, 3277–3280 (2006).
42. Massimini, M. *et al.* Breakdown of cortical effective connectivity during sleep. *Science* **309**, 2228–2232 (2005).
43. Khayat, P.S., Spekreijse, H. & Roelfsema, P.R. Attention lights up new object representations before the old ones fade away. *J. Neurosci.* **26**, 138–142 (2006).
44. Roelfsema, P.R., Tolboom, M. & Khayat, P.S. Different processing phases for features, figures and selective attention in the primary visual cortex. *Neuron* **56**, 785–792 (2007).
45. Bentin, S., Allison, T., Puce, A., Perez, E. & McCarthy, G. Electrophysiological studies of face perception in humans. *J. Cogn. Neurosci.* **8**, 551–565 (1996).
46. Bradley, M.M., Miccoli, L., Escrig, M.A. & Lang, P.J. The pupil as a measure of emotional arousal and autonomic activation. *Psychophysiology* **45**, 602–607 (2008).
47. Delorme, A. & Makeig, S. EEGLAB: an open source toolbox for analysis of single-trial EEG dynamics including independent component analysis. *J. Neurosci. Methods* **134**, 9–21 (2004).
48. Nikouline, V., Ruohonen, J. & Ilmoniemi, R.J. The role of the coil click in TMS assessed with simultaneous EEG. *Clin. Neurophysiol.* **110**, 1325–1328 (1999).
49. Towle, V.L. *et al.* The spatial location of EEG electrodes: locating the best-fitting sphere relative to cortical anatomy. *Electroencephalogr. Clin. Neurophysiol.* **86**, 1–6 (1993).

Task-specific signal transmission from prefrontal cortex
in visual selective attention

Yosuke Morishima, Rei Akaishi, Yohei Yamada, Jiro Okuda, Keiichiro Toma, Katsuyuki Sakai

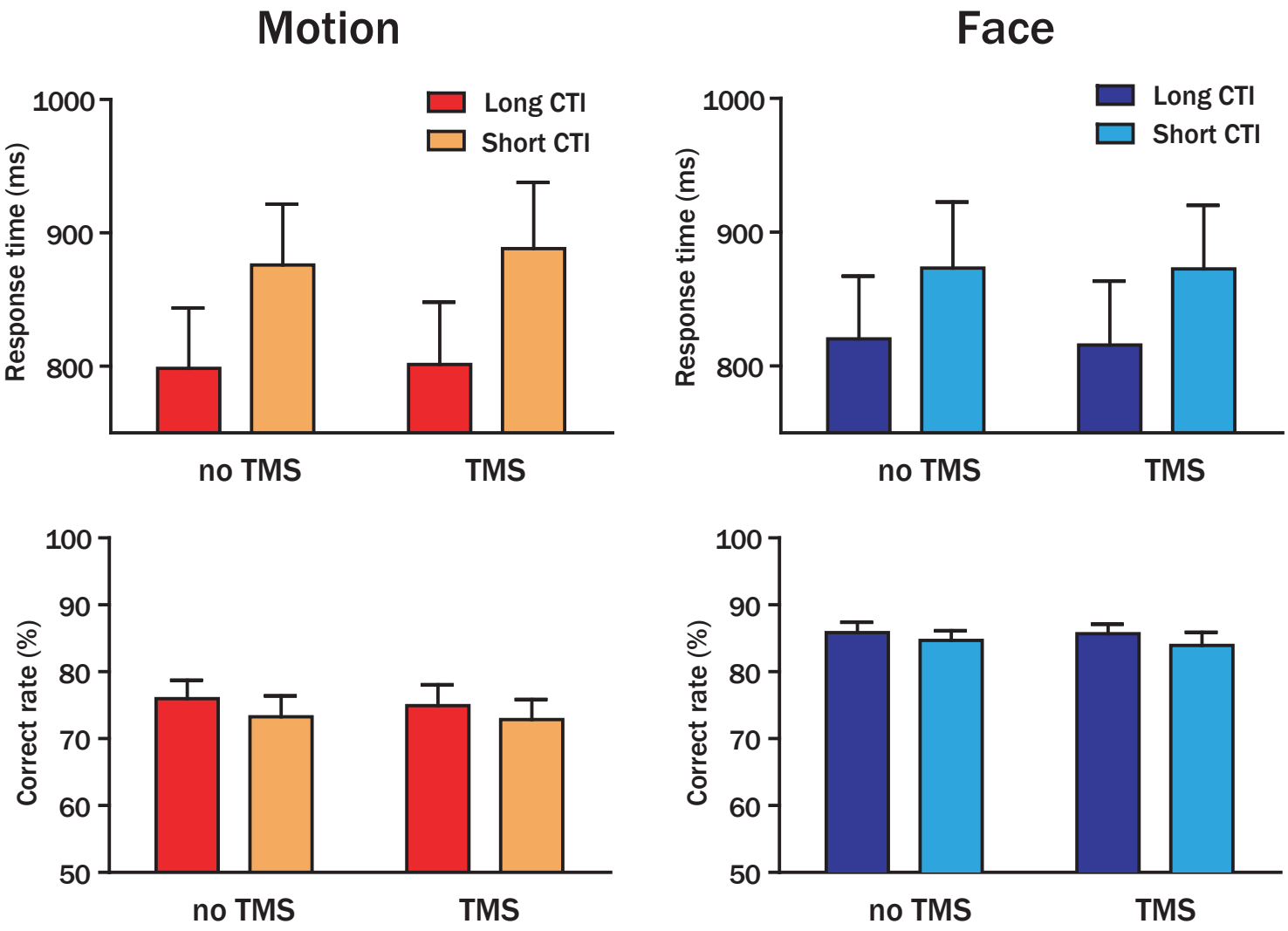

Supplementary Fig. 1

Behavioral results. Mean response time and correct rate are plotted for the long and short CTI trials in the motion and face conditions. Error bars indicate s.e.m.

Nature Neuroscience: doi:10.1038/nn.2237

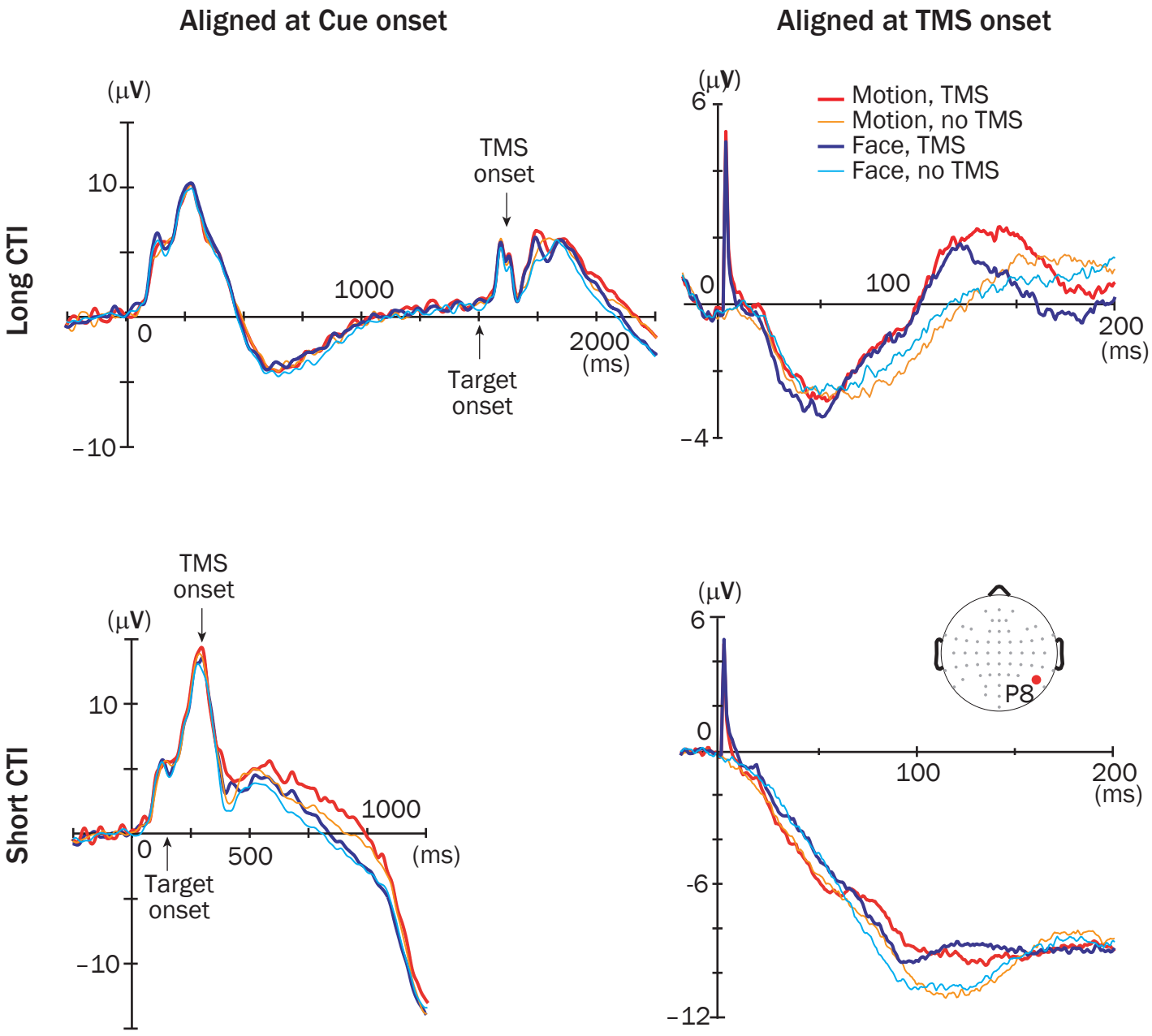

Supplementary Fig. 2

Single-condition ERP waveforms from the electrode P8 on the scalp separately shown for the long (upper panels) and short CTI trials (bottom panels). On the left are shown the waveforms for the whole task epoch, aligned at the onset of the task cue. On the right are shown the waveforms for the 200 ms epoch from the TMS onset, aligned at the TMS onset.

Nature Neuroscience: doi:10.1038/nn.2237

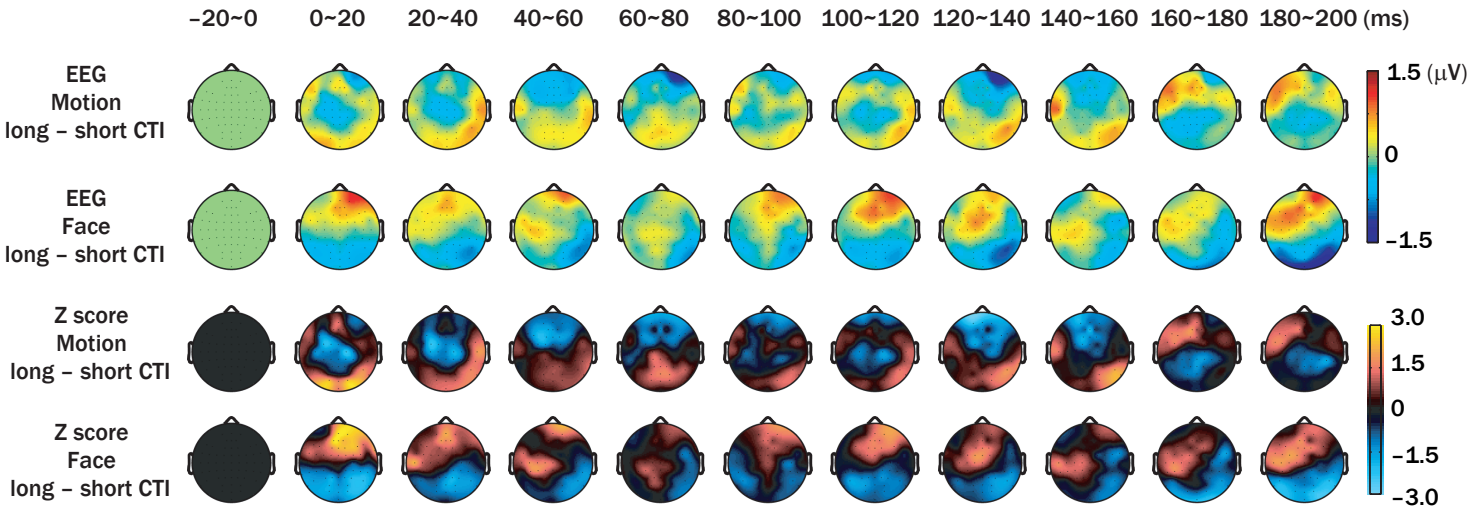

Supplementary Fig. 3

Mean voltage and z-score scalp maps for the differential TMS-induced ERPs between long and short CTI trials as in Fig. 3, but are now shown for the time period from –20 to 200 ms after the TMS. Top two rows show the difference in the mean voltage of TMS-induced ERPs for the contrast of the long minus short CTI trials. Bottom two rows show the z-scores for the contrast. The positive sign of the z-scores indicates more positive potential on the long CTI compared to short CTI trials.

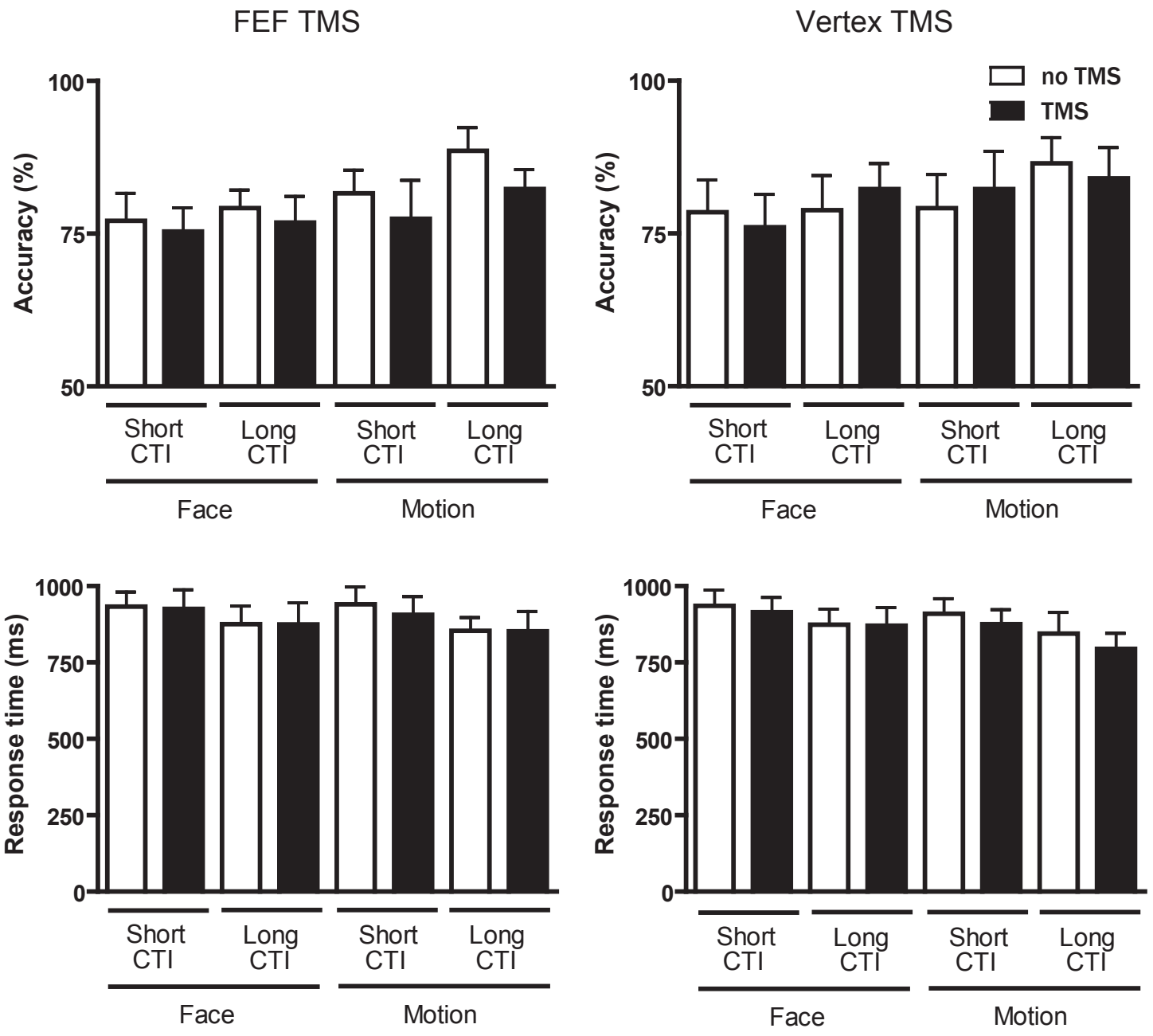

Supplementary Fig. 4

Perturbation of the FEF impairs feature discrimination. Accuracy (upper panel) and mean response time (lower panel) of the performance of feature discrimination task are plotted separately for the long and short CTI trials in the motion and face conditions with or without high-intensity double-pulse TMS. Left and right panels represent FEF TMS and vertex TMS sessions, respectively. Error bars indicate s.e.m. The TMS on the FEF significantly affected the accuracy of the performance relative to the no-TMS trials in the same session ($F(1, 5) = 18$, $p = 0.008$) but did not affect the response time significantly ($F(1, 5) = 0.43$, $p = 0.54$). However it did affect the shortening of the response times on long CTI trials relative to the short CTI trials (see main text and Fig. 5 for the effect on the preparation effect).

Nature Neuroscience: doi:10.1038/nn.3237

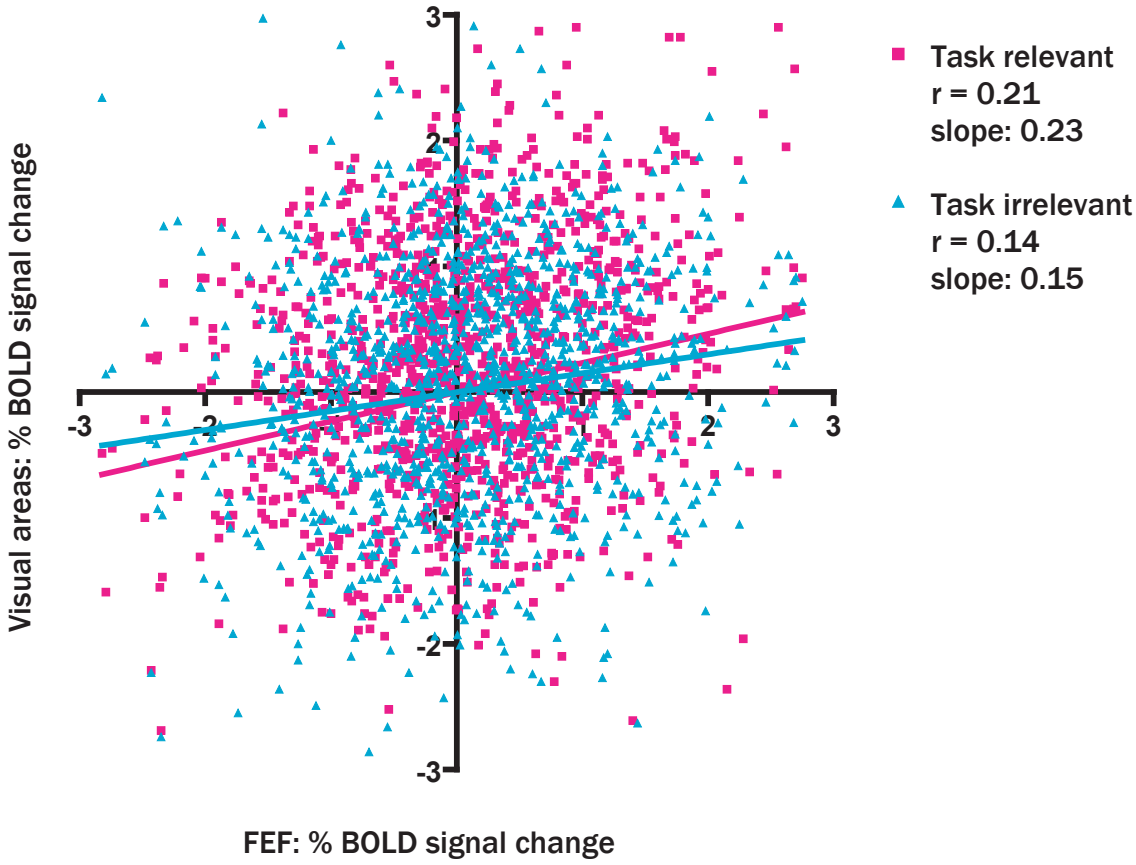

Supplementary Fig. 5

Functional connectivity analysis during the motion and face discrimination task based on fMRI experiments as described in the supplementary text. The signals in the task-relevant (pink) and task-irrelevant (cyan) visual areas are plotted against the signals in the FEF. The thick oblique line on the panel indicates the estimated linear regression line.

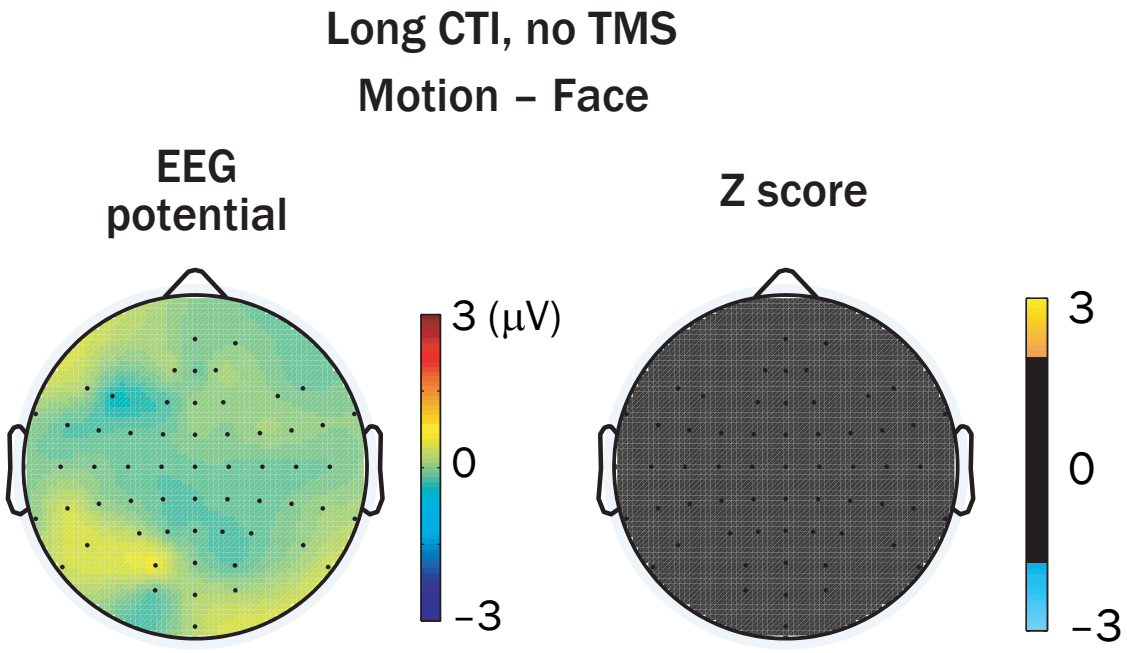

Supplementary Fig. 6

Difference in the scalp potentials (left) and z-score map representing the difference (right) between face and motion conditions on no TMS trials. The topographies are computed based on the data during 154–174 ms after the target onset, which corresponds to the time window of 20–40 ms after TMS on TMS trials. The z-score did not reach a significance level ($p < 0.05$) for all the electrodes.

SUPPLEMENTARY DATA

For five of the fifteen subjects we also conducted fMRI experiments using the same cued discrimination task for motion and face. In this experiment we used a mini-block design, where four trials were given in succession after a single task cue. Imaging was performed using a 1.5 tesla scanner (Sonata; Siemens, Erlagen, Germany). The functional images sensitive to blood oxygenation level-dependent (BOLD) contrasts were acquired by T2*-weighted echo planar imaging [repetition time, 2.1 s; echo time, 40 ms; 450 sequential whole-brain volume acquisition; in-plane resolution of 3 mm in 64 x 64 matrix; 25 slices; slice thickness of 5 mm; no interslice gap]. We used SPM2 for image data preprocessing and analysis. First five volumes were discarded, and remaining 445 volumes are realigned to first image, and normalized to the standard brain of the Montreal Neurological Institute. The data were spatially smoothed with a Gaussian kernel of full-width half-maximum at 8 mm. Statistical parametric maps of t-statistics were calculated for condition specific effects within a general linear model. For each motion and face task, task epoch was modeled as a box-car regressor starting from the onset of task cue to the end of the last trial in the block (duration 12.5 sec). All epochs were convolved with a canonical hemodynamic response function. The data were high-pass filtered with a

Nature Neuroscience: doi:10.1038/nn.2237

frequency cut-off at 100 s.

We performed conjunction analysis across the subjects to look for activations common to the subjects. By comparing motion and face tasks, we found a significant increase of activation, peaked at coordinate (56, –68, 8) for motion task ($t = 6.54$, $p < 0.005$) and (46 –54 –20) for face task ($t = 16.33$, $p < 0.0001$). These were nearly identical to the peak coordinates of the current source density analysis in the main experiment and thus were called MT and FFA, respectively. We also found that a region just anterior to the precentral gyrus at coordinate (46, 6, 60) show significant activation relative to the baseline for both the motion and face conditions ($t = 5.93$, $p < 0.005$). This region corresponds to the ventral portion of the FEF. To examine the functional connectivity between the FEF and the task-specific posterior visual areas, MT and FFA, we extracted BOLD signal time series from 4 mm spherical region of interest (ROI) around the peak coordinates identified by the across-subject analysis and normalized the time series for each ROI and subject. We used the data between 5 and 17.5 seconds after the onset of a task cue in order to account for the delay of the hemodynamic response. We then calculated the correlation coefficient (Pearson's r) of the signals between the FEF and posterior visual areas that are relevant for the task at hand (MT for motion task and FFA for face task). We also calculated the

Nature Neuroscience: doi:10.1038/nn.2237

correlation coefficient between the FEF and posterior visual areas that are irrelevant for the task at hand (FFA for motion task and MT for face task). The correlation coefficient was significantly larger between the FEF and task-relevant areas than between the FEF and task-irrelevant areas (0.21 vs. 0.14, $p = 0.012$) (**Supplementary Fig. 5**). Also the slope of the regression line was significantly higher between the FEF and task-relevant areas than between the FEF and task-irrelevant areas (0.23 vs. 0.15, $p = 0.041$). The results indicate task-specific changes in the pattern of functional connectivity between the FEF and posterior visual areas, but unlike the TMS-induced activation described in the main text the results of the fMRI experiment do not necessarily indicate that the FEF modulates the activity in posterior regions.